Chapter 2

Study of thermo-elastic cruciform crack with unequal arms in an orthotropic elastic plane

2.1 Introduction

The applications of fracture mechanics have traditionally concentrated on crack growth problems under an opening or mode-I mechanism. Damage tolerance is an ability of the structure due to which it sustains the defects until repair. During design of engineering structures, the damage tolerance is always taken in account as it is assumed that flaws can exist in any structure and such flaws propagate with usage. In aerospace engineering structures, this approach is necessarily used in aerospace

engineering structures to avoid the extension of cracks. It is observed in fracture mechanics that the crack growth is exponential in nature i.e., the crack growth rate is a function of an exponent of crack size. Due to exponential crack growth, the structural engineers may inspect invisible cracks occur in structures which may grow slowly by using non-destructive testing methods. Due to non-destructive inspections the amounts of maintenance checks can be reduced. Crack propagation and arrest have become important topics in a structure containing isolated region of an unstable crack growth. The emergence of an unstable crack can be arrested from bad region by using the surrounding of good materials, provided good materials have sufficiently high fracture toughness i.e., materials have large resistance to protect the structure from crack propagation. This clearly exhibits the importance of studying propagation of cracks occur in structures and the arrest of crack propagation for the sake of safety of the structure. Akoz and Tauchert (1972) have done a significant work in this field. Mishra *et al.* (2016) have studied the interaction among the interfacial cracks bonded between orthotropic elastic strips and half planes. Sneddon (1946) had studied the distribution of stress and displacement in an isotropic media.

During last few years, the thermo-elastic crack problems are been attracted by the scientists and engineers around the world. There has been increasing interest for the solution of elasto-static and elasto-dynamic crack problems in an anisotropic medium due to their important applications in space crafts, solar panels, racing car bodies, storage tanks *etc.* Due to mathematical complexity, comparatively few investigations of thermal stresses in anisotropic bodies have been appeared. Nowadays, macroscopic anisotropic constructions material like fiber reinforced composite are widely used in thermal environment. In this case determination of the thermal stress intensity around the crack become important, this occurs due to the disturbance in heat flux. Sometimes it is also seen that thermal stresses occur, due to

a sudden change in temperature of the structure, and thus combined with the effect of existing mechanical loads. Meanwhile crack-like defect may cause fracture under this thermo-mechanical stress. The investigation of thermo-elastic field and thermal stress concentration around the crack help to understand the stability and life of the cracked engineering materials and structures. According to linear elastic fracture mechanics stress at the vicinity of the crack tip is singular. It is directly proportional to the inverse of square root of distance from the crack tip. Many observations of thermo-elastic cracked surfaces show that the thermal stress singularity at the vicinity of the crack tips are same as those with mechanical stresses.

Initially in fracture mechanics cruciform specimen would be used to calculate the effect of biaxial load on stable crack growth during experimental tests and due to low cost towards manufacturing process the thick reduction of the cracks specimens was not been considered during modelling. During experiments, it is important to find the stress distribution and its intensity of cruciform specimen due to its complicated shape. Thus during configuration handling of cruciform cracks specimen, one should be careful about the facts that the specimen should be capable of taking compression load, the stress distribution across the specimen should be uniform and for minimizing the machining cost the specimen configuration should be simple. Different types of specimens and fatigue testing mechanics have been developed by the scientists and engineers. The two different kinds of specimen one as a large specimen at lower test level and another small specimen at a higher stress level were used for biaxial fatigue test by Miller (1982). In the year 2000, Kalluri and Bonacuse (2000) have used three different types of cruciform specimens on the DLR biaxial testing for investigation of fatigue and deformation towards easy monitoring and low manufacturing cost.

Stallybrass (1970), Rooke and Sneddon (1969), and Sneddon and Das

(1971) have studied the elasto-static cruciform crack and star shaped crack in isotropic elastic material by using different approaches, e.g., Integral transform technique, Wiener-Hopf technique and Muskhelishivilli-Kolsov potential functions, *etc.* The study of dynamic cruciform crack problem was done by Ong *et al.* (1985) and Brock *et al.* (1985) in an isotropic elastic medium. The T-stress, which plays an important role in determining crack growth direction and in changing apparent fracture toughness, was analyzed near the tips of cruciform cracks embedded in an isotropic elastic solid by Li (2006). But further research had been required to study the crack problems in an anisotropic medium with cruciform specimen. Several investigators have studied the cruciform crack problems by using different methods. In 1991, Zhang (1991) gave the general solution of a cruciform crack in orthotropic infinite plate under arbitrary longitudinal shear stress. The stability of the growth regime of cruciform crack was studied by Keer *et al.* (1980). De and Patra (1992) and Das *et al.* (2000) have solved the problem of a cruciform crack in an orthotropic elastic plane by using integral transform technique.

But to the best of my knowledge, the problem related to cruciform cracks under thermo-mechanical loading are not yet been solved by any researcher by using orthogonal Chebyshev polynomials. The stress intensity factors at the tips of the cracks and crack energies are found analytically. The numerical computations of the stress magnification factors to find the possibilities of shielding and amplification of cracks through the stress magnification factors and requirement of energy for fracture toughness are the key features of the present chapter.

This chapter deals with elasto-static cruciform crack with prescribed thermo-mechanical loading embedded in an orthotropic elastic plane. A steady state temperature field induced by a line source is situated at the origin of the cruciform crack. Integral transform technique has been used to reduce the pair of Fredholm

type singular integral equations, which are finally been solved by using Chebyshev polynomials. The analytical expressions of the stress intensity factors at the tips of two arms and the crack energies towards finding the toughness of the material are found. The numerical values of stress magnification factors and the dimensionless quantities of crack energies are computed for Boron-Epoxy composite material for different particular cases which are depicted through graphs.

2.2 Problem Formulation

Consider the elasto-static plane problem in an infinite orthotropic thermo-elastic medium containing a cruciform crack on the segment $|x| \leq a$, $y = 0$ and $|y| \leq b$, $x = 0$ when Cartesian co-ordinate axes coincide with the axes of symmetry of the elastic material. When thermal conditions are applied to the surface of an arbitrary two dimensional orthotropic media then temperature field only depends upon in-plane co-ordinates under steady state condition. Thus, the temperature distribution functions $T(x, y)$ are assumed to satisfy the following heat conduction equation in the orthotropic media as

$$\frac{\partial^2 T}{\partial x^2} + K^2 \frac{\partial^2 T}{\partial y^2} = 0, \tag{2.1}$$

where $K^2 = K_y/K_x$ with K_y, K_x are the thermal conductive coefficients of the orthotropic material along y and x directions, respectively.

The general solution of $T(x, y)$ is (c.f., Akoz and Tauchert (1972))

$$T(x, y) = \frac{1}{2\pi} \int_0^\infty \left[A(p) exp\left\{ p\left(ix - \frac{y}{K} \right) \right\} + \bar{A}(p) exp\left\{ p\left(-ix - \frac{y}{K} \right) \right\} \right] dp, \tag{2.2}$$

where $i = \sqrt{-1}$, $j = 1, 2$, and $A(p)$ and $\bar{A}(p)$ are the arbitrary functions of p.

Taking

$$T(x, 0) = h(x), \tag{2.3}$$

the Fourier integral form of temperature distribution becomes

$$T(x, 0) = \frac{1}{2\pi} \int_0^\infty \left[\int_{-\infty}^\infty h(\xi) \, exp[p(i\xi)] \, exp[p(ix)] \right.$$
$$\left. + h(\xi) \, exp[p(i\xi)] \, exp[p(-ix)] \, d\xi \right] dp. \tag{2.4}$$

From equations (2.2) and (2.4), we get

$$A(p) = \int_{-\infty}^\infty h(\xi) exp[-ip\xi] \, d\xi, \quad \bar{A}(p) = \int_{-\infty}^\infty h(\xi) exp[ip\xi] \, d\xi. \tag{2.5}$$

From equations (2.2) and (2.5), the temperature distribution $T(x, y)$ can be expressed as

$$T(x, y) = \frac{1}{\pi} \int_{-\infty}^\infty \frac{(\frac{y}{K}) h(\xi)}{(\frac{y}{K})^2 + (\xi - x)^2} \, d\xi. \tag{2.6}$$

If we consider

$$h(x) = \delta(x), \tag{2.7}$$

where the prescribed temperature distribution, $h(x)$ becomes line source along y-axis as Dirac delta function $\delta(x)$, the resultant temperature distribution is reduced to

$$T(x, y) = \frac{1}{\pi} \frac{(\frac{y}{K})}{(\frac{y}{K})^2 + x^2}. \tag{2.8}$$

The relations between plane stress induced by the distributions of temperature and displacement components u and v are given by

$$\sigma_{xx}(x,y) = C_{11}\frac{\partial u}{\partial x} + C_{12}\frac{\partial v}{\partial y} - \beta_x T, \tag{2.9}$$

$$\sigma_{yy}(x,y) = C_{12}\frac{\partial u}{\partial x} + C_{22}\frac{\partial v}{\partial y} - \beta_y T, \tag{2.10}$$

$$\sigma_{xy}(x,y) = C_{66}\left(\frac{\partial u}{\partial x} + \frac{\partial v}{\partial y}\right). \tag{2.11}$$

The elastic constants are given by $C_{11} = \frac{E_{xx}}{1 - v_{xy}v_{yx}}$, $C_{22} = \frac{E_{yy}}{1 - v_{xy}v_{yx}}$, $C_{12} = \frac{E_{yy}v_{xy}}{1 - v_{xy}v_{yx}} = \frac{E_{xx}v_{yx}}{1 - v_{xy}v_{yx}}$, $C_{66} = G_{xy}$ and stress-temperature coefficients are defined by $\beta_x = C_{12}\alpha_{yy} + C_{11}\alpha_{xx}$, $\beta_y = C_{12}\alpha_{xx} + C_{22}\alpha_{yy}$, where E_{xx}, E_{yy} are the Young's moduli, G_{xy} is shear modulus, v_{xy} and v_{yx} are Poisson's ratios, α_{xx} and α_{yy} are linear expansion coefficients. It is to be noted that the units of $C_{jk}^{(i)}$'s are taken as GPa and units of β_x and β_y are considered as GPa/deg.

The displacement equations of equilibrium are given by

$$C_{11}\frac{\partial^2 u}{\partial x^2} + C_{66}\frac{\partial^2 u}{\partial y^2} + (C_{12} + C_{66})\frac{\partial^2 v}{\partial x \partial y} = \beta_x\frac{\partial T}{\partial y}, \tag{2.12}$$

$$C_{22}\frac{\partial^2 v}{\partial y^2} + C_{66}\frac{\partial^2 v}{\partial x^2} + (C_{12} + C_{66})\frac{\partial^2 u}{\partial x \partial y} = \beta_y\frac{\partial T}{\partial y}, \tag{2.13}$$
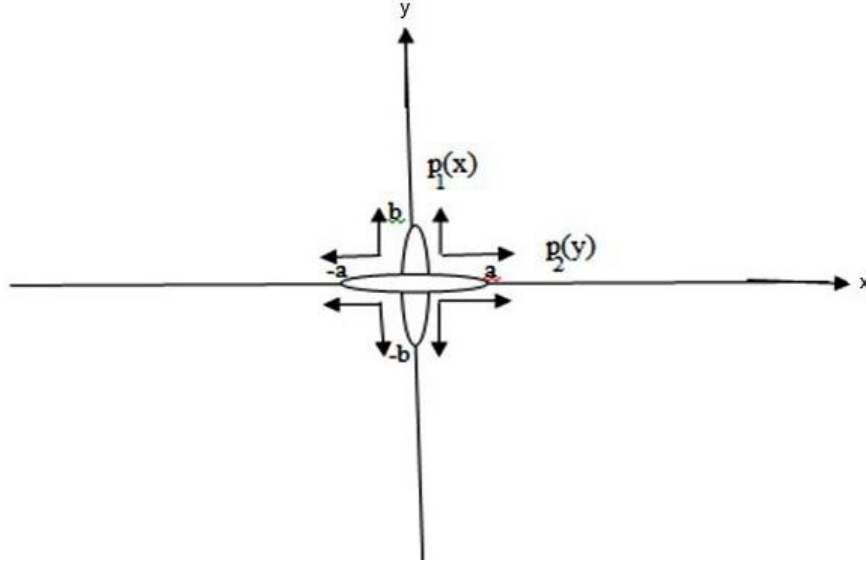
Figure 2.1: Geometry of the Problem

where $u = u(x,y)$, $v = v(x,y)$ are the displacement components along x and y directions. In view of symmetry, the problem can be formulated in the quarter-plane ($x \geq 0$, $y \geq 0$) associated with the boundary conditions given by

$$\sigma_{yy}(x,0) = -p_1(x), \qquad 0 \leq x \leq a, \qquad (2.14)$$

$$\sigma_{xx}(0,y) = -p_2(y), \qquad 0 \leq x \leq b, \qquad (2.15)$$

$$u(0,y) = 0, \qquad y > b, \qquad (2.16)$$

$$v(x,0) = 0, \qquad x > a, \qquad (2.17)$$

$$\sigma_{xy}(0,y) = 0, \qquad y \geq 0, \qquad (2.18)$$

$$\sigma_{xy}(x,0) = 0, \qquad x \geq 0, \qquad (2.19)$$

where $p_1(x)$ and $p_2(y)$ are internal tractions during opening of cracks and the overall geometry of the concerned model is provided in Figure 2.1.

2.3   Solution of the Problem

For solution of the problem, displacement potential functions $\psi(x,y)$ and $\phi_j(x,y)$ $(j=1,2)$ are taken as

$$\psi(x,y) = \frac{1}{2\pi}\int_0^\infty \left[A(s)B(s)e^{s\left\{ix-\left(\frac{y}{k}\right)\right\}} + \bar{A}(s)\bar{B}(s)e^{s\left\{-ix-\left(\frac{y}{k}\right)\right\}}\right] ds, \qquad (2.20)$$

$$\phi_1(x,y) = \frac{2}{\pi}\int_0^\infty \left[s^{-1}B_1(s)e^{-sx\sqrt{\mu_1}}\cos(sy) + s^{-2}C_1(s)e^{-\frac{sy}{\sqrt{\mu_1}}}\cos(sx)\right] ds, \quad (2.21)$$

$$\phi_2(x,y) = \frac{2}{\pi}\int_0^\infty \left[s^{-1}B_2(s)e^{-sx\sqrt{\mu_2}}\cos(sy) + s^{-2}C_2(s)e^{-\frac{sy}{\sqrt{\mu_2}}}\cos(sx)\right] ds. \quad (2.22)$$

The displacement components u and v may be written as

$$u = \frac{\partial\psi}{\partial x} + \frac{\partial\phi_1}{\partial x} + \frac{\partial\phi_2}{\partial x} \qquad \text{and} \quad v = \eta\frac{\partial\psi}{\partial y} + \lambda_1\frac{\partial\phi_1}{\partial y} + \lambda_2\frac{\partial\phi_2}{\partial y}.$$

The corresponding thermal stresses are

$$\frac{\sigma_{xx}(x,y)}{C_{66}} = -\left[(1+\lambda_1)\frac{\partial^2\phi_1}{\partial y^2} + (1+\lambda_2)\frac{\partial^2\phi_2}{\partial y^2} + (1+\eta)\frac{\partial^2\psi}{\partial y^2}\right], \qquad (2.23)$$

$$\frac{\sigma_{yy}(x,y)}{C_{66}} = \left[(1+\lambda_1)\mu_1\frac{\partial^2\phi_1}{\partial y^2} + (1+\lambda_2)\mu_2\frac{\partial^2\phi_2}{\partial y^2} - (1+\eta)\frac{\partial^2\psi}{\partial x^2}\right], \qquad (2.24)$$

$$\frac{\sigma_{xy}(x,y)}{C_{66}} = \left[(1+\lambda_1)\frac{\partial^2\phi_1}{\partial x\partial y} + (1+\lambda_2)\frac{\partial^2\phi_2}{\partial x\partial y} + (1+\eta)\frac{\partial^2\psi}{\partial x\partial y}\right]. \qquad (2.25)$$

The displacement equations (2.12)-(2.13) are satisfied by equation (2.20) for non-trivial ϕ_j if

$$\eta = \frac{\beta_y(C_{66} - K^2C_{11}) + \beta_x(C_{12} + C_{66})K^2}{\beta_x(C_{22} - K^2C_{66}) - \beta_y(C_{12} + C_{66})}, \qquad (2.26)$$

$$s^2B = s^2\bar{B} = K^2\frac{\beta_x(C_{22} - K^2C_{66}) - \beta_y(C_{12} + C_{66})}{(C_{22} - K^2C_{66})(C_{66} - K^2C_{11}) + K(C_{12} + C_{66})^2} = k, \qquad (2.27)$$

$$\frac{C_{66} + \lambda(C_{12} + C_{66})}{C_{11}} = \frac{\lambda C_{22}}{\lambda C_{66} + C_{12} + C_{66}} = \mu, \qquad (2.28)$$

where k, η are constant quantities. Equation (2.28) yields two quadratic equations, one in λ and the other in μ. λ_1, λ_2 and μ_1, μ_2 are the roots of the quadratic equations

$$C_{66}(C_{12} + C_{66})\lambda^2 + [(C_{12} + C_{66})^2 + C_{66}{}^2 - C_{11}C_{22}]\lambda + C_{66}(C_{12} + C_{66}) = 0,$$

and $\quad C_{11}C_{66}\mu^2 + [(C_{12} + C_{66})^2 - C_{66}{}^2 - C_{11}C_{22}]\mu + C_{22}C_{66} = 0.$

Here, $\mu_i(i = 1, 2)$ are associated with potential functions ϕ_i, which satisfy the following differential equations

$$\left(\frac{\partial^2}{\partial x^2} + \frac{\partial^2}{\partial y_i{}^2}\right)\phi_j(x, y) = 0, i = 1, 2; j = 1, 2, \tag{2.29}$$

where $y_i = \frac{y}{\sqrt{\mu_i}}, i = 1, 2.$

Applying the boundary conditions (2.18) and (2.19), we get

$$C_1(s) = -\frac{\sqrt{\mu_1}}{\sqrt{\mu_2}}\left(\frac{1 + \lambda_2}{1 + \lambda_1}\right)C_2(s) - \frac{k}{K}\frac{\sqrt{\mu_1}}{\pi}\left(\frac{1 + \eta}{1 + \lambda_1}\right), \tag{2.30}$$

$$B_1(s) = -\frac{\sqrt{\mu_2}}{\sqrt{\mu_1}}\left(\frac{1 + \lambda_2}{1 + \lambda_1}\right)B_2(s). \tag{2.31}$$

Applying the boundary conditions (2.16) and (2.17), we get

$$\int_0^\infty s^{-1}C_2(s)\cos(sx)ds = 0, x > a, \tag{2.32}$$

$$\int_0^\infty B_2(s)\cos(sy)ds = 0, y > b. \tag{2.33}$$

Boundary conditions (2.16) and (2.17) with the aid of equations (2.30) and (2.31) give arise to

$$\sqrt{\mu_2}\int_0^\infty sB_2(s)\left(\sqrt{\mu_1}e^{-\sqrt{\mu_2}sx} - \sqrt{\mu_2}e^{\sqrt{\mu_1}sx}\right)ds + \left(1 - \frac{\sqrt{\mu_1}}{\sqrt{\mu_2}}\right)$$
$$\int_0^\infty C_2(s)\cos(sx)ds = -p_1{}'(x), 0 \leq x \leq a, \tag{2.34}$$

$$\left(1 - \frac{\sqrt{\mu_2}}{\sqrt{\mu_1}}\right) \int_0^\infty sB_2(s)\cos(sy)ds + \frac{1}{\sqrt{\mu_2}} \int_0^\infty \left(\frac{e^{-\sqrt{\mu_2}sy}}{\sqrt{\mu_1}}\right.$$

$$\left. - \frac{e^{-\sqrt{\mu_1}sy}}{\sqrt{\mu_2}}\right) C_2(s)ds = p_2^{'}(x), 0 \le y \le b, \quad (2.35)$$

where

$$p_1^{'}(x) = \frac{\pi}{2}\frac{p_1(x)}{C_{66}(1+\lambda_1)} + \left(\frac{(1+\eta)k}{(1+\lambda_2)}\right)\left(\frac{1}{2\pi} - \frac{\sqrt{\mu_1}}{\pi K}\right)\delta(x),$$

Setting,

$$B_2(s) = \frac{1}{s}\int_0^a f_1(t)\sin(st)\,dt, \quad (2.36)$$

and

$$C_2(s) = \int_0^b f_2(\tau)\sin(s\tau)\,d\tau, \quad (2.37)$$

so that the equations (2.32) and (2.33) are satisfied under the following conditions

$$\int_{-a}^a f_1(t)dt = 0 \text{ and } \int_{-b}^b f_2(\tau)d\tau = 0. \quad (2.38)$$

After lengthy process of mathematical calculations, the equations (2.34) and (2.35) with the aid of equations (2.36) and (2.37) along with the compatibility conditions (2.38) finally lead to the following singular integral equations:

$$\beta_1 \int_{-a}^a \frac{f_1(t)}{(t-x)}\,dt + \int_0^a k_1(x,\tau)f_2(\tau)\,d\tau$$

$$= -\frac{p_1(x)}{C_{66}(1+\lambda_1)} - \left(\frac{(1+\eta)k}{(1+\lambda_2)}\right)\left(\frac{1}{2\pi} - \frac{\mu_1}{\pi K}\right)\delta(x), -a \le x \le a, \quad (2.39)$$

$$\beta_2 \int_{-b}^b \frac{f_2(\tau)}{(\tau-y)}\,d\tau + \int_0^b k_2(y,t)f_1(t)\,dt$$

$$= -\frac{p_2(x)}{C_{66}(1+\lambda_1)} - \left(\frac{(1+\eta)k}{(1+\lambda_2)}\right)\left(\frac{1}{\pi} - 1\right), -b < x < b, \quad (2.40)$$

where

$$\beta_1 = \frac{1}{2}\left(1 - \frac{\sqrt{\mu_1}}{\sqrt{\mu_2}}\right), \beta_2 = \frac{1}{2}\left(1 - \frac{\sqrt{\mu_2}}{\sqrt{\mu_1}}\right),$$

$$k_1(x,\tau) = \sqrt{\mu_2}\left(\frac{\sqrt{\mu_1}\tau}{\mu_1 x^2 + \tau^2} - \frac{\sqrt{\mu_2}\tau}{\mu_2 x^2 + \tau^2}\right),$$

$$k_2(y,\tau) = \frac{1}{\sqrt{\mu_2}}\left(\frac{\sqrt{\mu_1}t}{y^2 + \mu_1 t^2} - \frac{\sqrt{\mu_2}t}{y^2 + \mu_2\tau^2}\right).$$

Putting the variables $x^* = x/a$, $y^* = y/b$, $t^* = t/a$, $\tau^* = \tau/b$, the above integral equations are reduced to

$$\beta_1 \int_{-1}^{1} \frac{f_1(t^*)}{(t^* - x^*)}dt + \int_{0}^{1} k_1(x^*,\tau^*)f_2(\tau^*)d\tau^* = -p_1^{''}(x^*), -1 \le x^* \le 1, \quad (2.41)$$

$$\beta_2 \int_{-1}^{1} \frac{f_2(\tau^*)}{(\tau^* - y^*)}d\tau^* + \int_{0}^{1} k_2(y^*,t^*)f_1(t^*)dt^* = -p_2^{''}(y^*), -1 \le y^* \le 1, \quad (2.42)$$

where

$$p_1^{''}(x^*) = \frac{p_1(x^*)}{C_{66}(1 + \lambda_1)} + \left(\frac{(1+\eta)k}{(1+\lambda_2)}\right)\left(\frac{1}{2\pi} - \frac{\sqrt{\mu_1}}{\pi K}\right)\delta(x^*),$$

$$p_2^{''}(y^*) = \frac{p_2(y^*)}{C_{66}(1 + \lambda_1)} + \left(\frac{(1+\eta)k}{(1+\lambda_2)K}\right)\left(\frac{1}{\pi} - 1\right),$$

with

$$\int_{-1}^{1} f_1(t^*)dt^* = 0 \text{ and } \int_{-1}^{1} f_2(\tau^*)d\tau^* = 0. \quad (2.43)$$

Now expressing the unknown functions $f_1(t^*)$ and $f_2(\tau^*)$ in terms of Chebyshev polynomials of first kind as

$$f_1(t^*) = \frac{1}{\sqrt{(1 - t^{*2})}}\sum_{n=0}^{\infty} A_n T_{2n+1}(t^*),$$

$$f_2(\tau^*) = \frac{1}{\sqrt{(1 - \tau^{*2})}}\sum_{n=0}^{\infty} B_n T_{2n+1}(\tau^*), \quad (2.44)$$

and use the following orthogonal relations of Chebyshev polynomials

$$\int_{-1}^{1} T_j(t^*)(1-t^{*2})^{-\frac{1}{2}}\frac{dt^*}{(t^*-x^*)} = \begin{cases} 0, & j=0, \\ \pi\, U_{j-1}(x^*), & j>0, \end{cases}$$

$$\int_{-1}^{1} U_n(y^*)U_m(y^*)(1-y^{*2})^{\frac{1}{2}}dy^* = \begin{cases} 0, & n \neq m, \\ \frac{\pi}{2}, & n=m. \end{cases}$$

The equations (2.41) and (2.42) are reduced to the system of linear algebraic equations in terms of unknown coefficients A_n and B_n as

$$A_m\left(\frac{\pi^2\beta_1}{2}\right) + \sum_{n=0}^{\infty} B_n \int_{-1}^{1} U_{2n}(x^*)\sqrt{1-x^{*2}}dx^*$$
$$\left(\int_0^1 k_1(x^*,\tau^*)T_{2n+1}(\tau^*)d\tau^*\right) = -\frac{1}{\theta}P_{1m}, \quad (2.45)$$

$$B_m\left(\frac{\pi^2\beta_2}{2}\right) + \sum_{n=0}^{\infty} A_n \int_{-1}^{1} U_{2n}(y^*)\sqrt{1-y^{*2}}dy^*$$
$$\left(\int_0^1 k_2(y^*,t^*)T_{2n+1}(t^*)dt^*\right) = -\frac{1}{\theta}P_{2m}, \quad (2.46)$$

where $P_{1m} = \int_{-1}^{1}(p_1''(x^*))U_{2m}(x^*)\sqrt{1-x^{*2}}dx^*$,

$P_{2m} = \int_{-1}^{1}(p_2''(y^*))U_{2m}(y^*)\sqrt{1-y^{*2}}dy^*, \quad \theta = C_{66}(1+\lambda_2)$.

The stress intensity factors at the cruciform crack tips $x = a$ and $y = b$ are calculated as

$$K_a = \lim_{x\to a^+}\sqrt{2(x-a)}\sigma_{yy}(x,0) = -\theta\beta_1\left[\sum_{n=0}^{\infty} A_n\right], \quad (2.47)$$

$$K_b = \lim_{y\to b^+}\sqrt{2(y-b)}\sigma_{xx}(0,y) = -\theta\beta_2\left[\sum_{n=0}^{\infty} B_n\right]. \quad (2.48)$$

Expressions of the crack energies for both the cracks are given as

$$
\begin{aligned}
W_1 &= -2 \int_0^a \sigma_{yy}(x,0)v(x,0)dx \\
&= -\frac{\pi(\lambda_1 - \lambda_2)}{2\delta_2(1+\lambda_1)} \sum_{n=0}^{\infty} A_n \int_{-1}^{1} \frac{T_{2n+1}(t^*)dt^*}{\sqrt{(1-t^{*2})}} \int_{-1}^{t^*} \Bigg(p_1(x^*) \\
&\qquad + \left(\frac{(1+\eta)k}{(1+\lambda_2)} \right) \left(\frac{1}{2\pi} - \frac{1}{K} \right) \delta(x^*) \Bigg) dx^*, \quad (2.49)
\end{aligned}
$$

$$
\begin{aligned}
W_2 &= -2 \int_0^b \sigma_{xx}(0,y)u(0,y)dy \\
&= -\frac{\pi(\lambda_1 - \lambda_2)\delta_2}{2(1+\lambda_1)} \sum_{n=0}^{\infty} B_n \int_{-1}^{1} \frac{T_{2n+1}(\tau^*)d\tau^*}{\sqrt{(1-\tau^{*2})}} \int_{-1}^{\tau^*} \Bigg(p_2(y^*) \\
&\qquad + \left(\frac{(1+\eta)k}{(1+\lambda_2)y^*} \right) \left(\frac{1}{K\pi} - 1 \right) \Bigg) dy^* \quad (2.50)
\end{aligned}
$$

The stress magnification factors (SMF) and the ratios of crack energies for both the arms of the crack are given by

$$
M_a = \frac{K_a}{K_a^*}, \ M_b = \frac{K_b}{K_b^*}, \ W_1^* = \frac{W_1}{W_{1a}} \ \text{and} \ W_2^* = \frac{W_2}{W_{2b}},
$$

where K_a^* and K_b^* are respectively the stress intensity factors at $x = a$ due to presence of horizontal crack ($b/a \to 0$) and at $x = b$ due to presence of vertical crack ($b/a \to \infty$). W_{1a} and W_{2b} are respective crack energies.

2.4　Results and Discussion

In this section the stress intensity factors K_a and K_b, the crack energies W_1 and W_2 have been calculated for a cruciform crack embedded in orthotropic medium viz., Boron-epoxy composite whose material constants are taken as
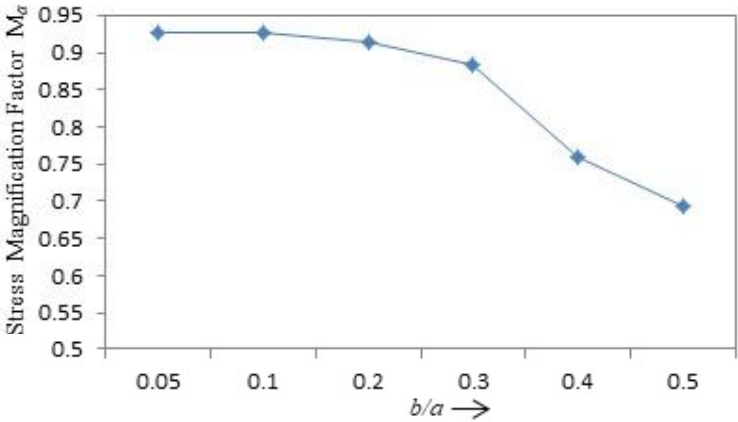
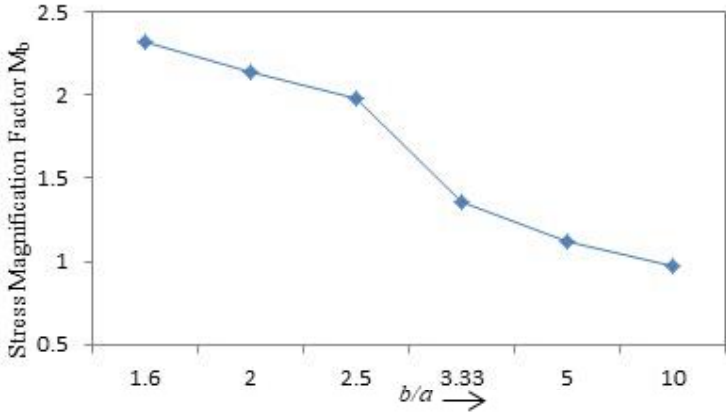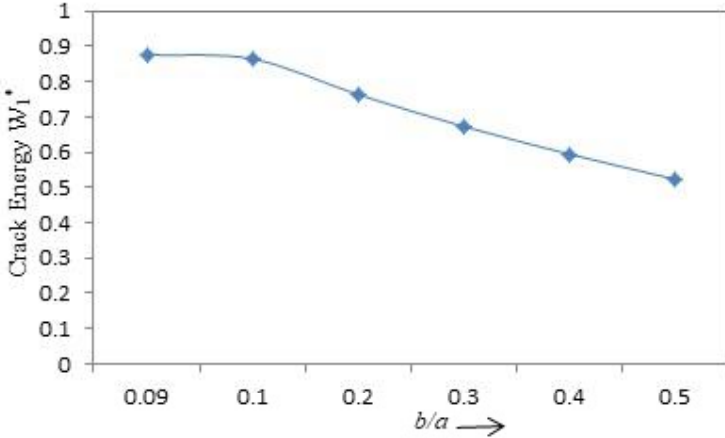**Figure 2.2:** Plots of M_a versus b/a.

Figure 2.3: Plots of M_b versus b/a.
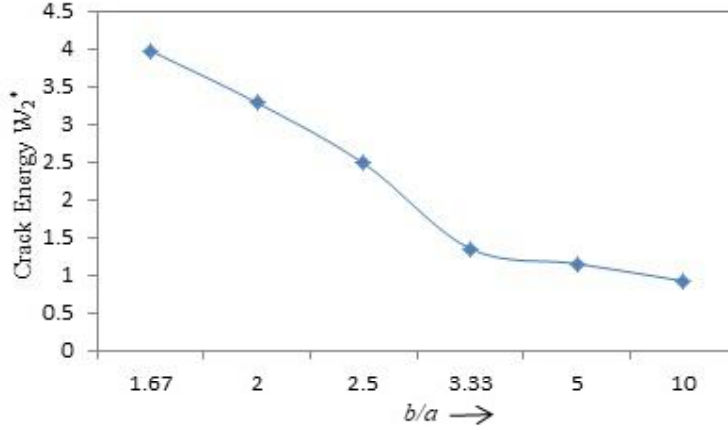

Figure 2.4: Plots of W_1^* versus b/a.

Figure 2.5: Plots of W_2^* versus b/a.

$C_{11} = 30.3 \times 10^6 \text{psi} \,(208.91 \,\text{GPa})$, $C_{12} = 3.78 \times 10^6 \text{psi} \,(26.06 \,\text{GPa})$, $C_{22} = 4.04 \times 10^6 \text{psi} \,(27.85 \,\text{GPa})$, $C_{66} = 1.13 \times 10^6 \text{psi} \,(7.79 \,\text{GPa})$, $K = 1.6$, $\beta_y/\beta_x = 1.6$ with $p_1(x) = p$, $p_2(y) = p$.

During numerical computation of M_a, the horizontal crack length is fixed as $a = 1$ and vary the value of b as $b = 0.1(0.1)0.5$. During computation of M_b, the vertical crack length is kept fixed as $b = 1$ and varying the value of a as $a = 0.1(0.1)0.5$. It is seen from Figure 2.2 that as b/a increases M_a decreases. The decrease of M_a with the increase of b/a shows the shielding phenomenon i.e., there is no possibility of crack propagation. It is seen from Figure 2.3 that as b/a increases M_b decreases, it is due to increase of crack length $2a$ and M_b increases with increase of crack length $2b$ which shows the amplification phenomenon i.e., there is a possibility of crack propagation and it will be started after attaining its critical value. It is also observed from Figure 2.2 that as b/a approaches to zero, the concerned problem seems to be a line crack along x-axis. Therefore, the stress magnification factor M_a at the crack tip $x = a$ of the horizontal crack approaches to unity. For Figure 2.3, as b/a approaches to large value then the model will be reduced to a line crack along y-axis and the stress magnification factor at the crack tip $x = b$ of the vertical crack

approaches to unity.

Figure 2.4 and Figure 2.5 represent the variations of ratios crack energies W_1^* and W_2^* against b/a for different particular cases. It is seen from the Figures that W_1^* and W_2^* decrease with the increase of b/a and W_1^* approaches to unity as b/a approaches to zero while W_2^* approaches to unity for large values of b/a. This will resist the crack tips to propagate. This means with the increase in horizontal crack arm compared vertical crack crack arm, there is a possibility of arrest of the crack propagation.

2.5　Conclusion

Through the present study, the author has achieved three important goals. First one is finding the expressions of SMF for cruciform crack under thermo-mechanical loading in an infinite orthotropic elastic medium. Second one is exhibition of the graphical presentations of possibilities of crack arrest and also crack propagation for various values of the cruciform crack specimen. Third one is the extraction and the graphical presentations of crack energy for different particular cases. The author is optimist that the proposed model will be beneficial for the researchers and engineers working in the field of composite medium with cruciform and star shaped cracks.

****